Complementary Aerodynamic Performance Datasets for Variable Speed Power Turbine Blade Section from Two Independent Transonic Turbine Cascades

The 22nd International Symposium on Air Breathing Engines
ISABE2015-20163
Phoenix, Arizona
October 25-30, 2015

Ashlie B. Flegel, NASA Glenn Research Center
Gerard E. Welch, NASA Glenn Research Center
Paul W. Giel, Vantage Partners, LLC
Forrest E. Ames, University of North Dakota
Jonathon A. Long, University of North Dakota

Motivation for VSPT Technology

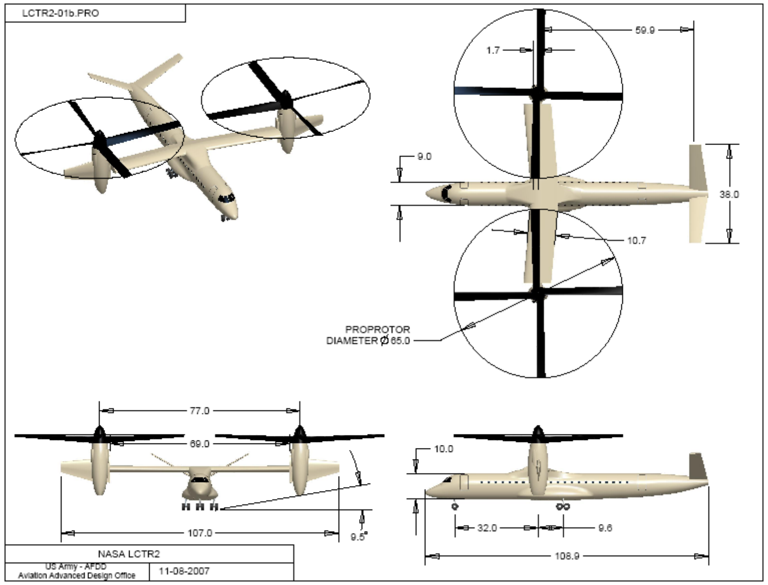

Acree, Hyeonsoo, and Sinsay, Int. Powered Lift Conf., 2008.

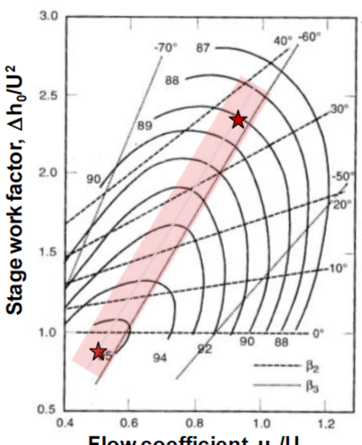

Smith chart

Large Civil Tilt-Rotor	
TOGW	108k lbm
Payload	90 PAX
Engines	4 × 7500 SHP
Range	> 1,000 nm
Cruise speed	> 300 kn
Cruise altitude	28 – 30 kft

Principal Challenge

Variability in main-rotor speed:
– 650 ft/s VTOL
– 350 ft/s at *Mn* 0.5 cruise

≈10 pts. in η_{prop}

Approaches

– Variable gear-ratio transmission
– Variable-speed power turbine **(VSPT)**
– or combination

VSPT Challenges

– Efficiency at high cruise work factor
- $\Delta h_0 = \Delta(u_q \cdot U) \approx$ const. at cruise and takeoff
- $\Delta h_0/U^2$ cruise is 3.5 × takeoff

– 40° to 60 ° incidence angle variations in all blade row (and EGV) with 50% speed change

– Operation at low *Re* – transitional flow
- 28 to 30 k-ft cruise leads to 60 k < $Re_{cx,2}$ < 100 k
- Transitional flow

VSPT Approach and Objectives

- Document blade performance over wide incidence angle range, a wide Reynolds number range, and at mission-relevant Mach numbers.
  - NASA's initial test conducted at low inlet turbulence in order to admit transitional flow.
  - NASA subsequently repeated tests at higher, engine-relevant inlet *Tu* (8%-15%).
- UND facility smaller scale, able to achieve lower Reynolds numbers.
- UND also measured blade surface heat transfer for transition locations.

$$Cp_s = \frac{P - \overline{P_2}}{P_{t,1} - \overline{P_2}}$$

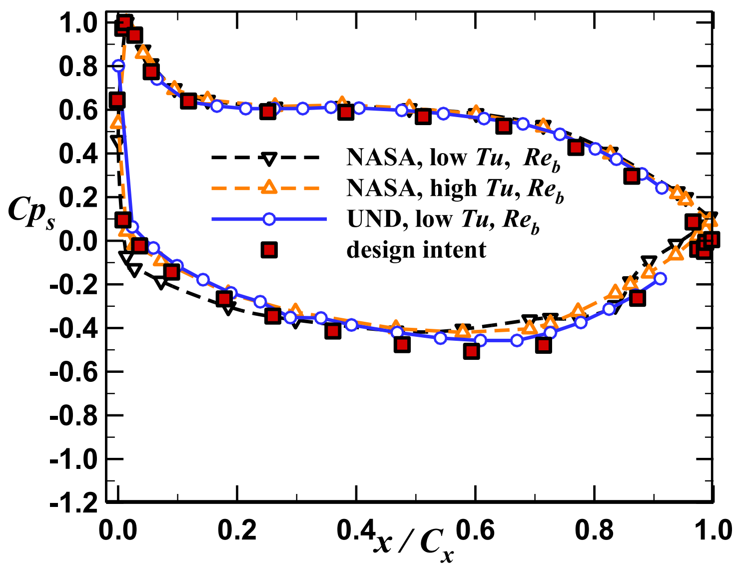

Design Intent Blade Loading and Experimental Data at $i = +5.8°$

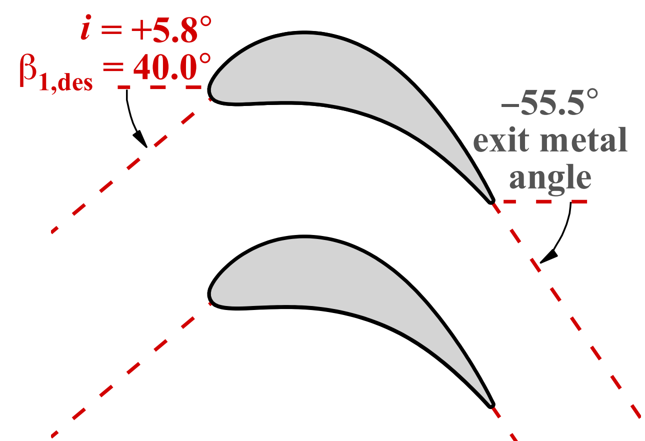

Blade Details	
Stagger angle	20.4°
Uncovered turning	19.5°
Zweifel coefficient, Zw_{des}	1.06
Solidity, $C_x / Pitch$	1.39

NASA Facility Operating Envelope

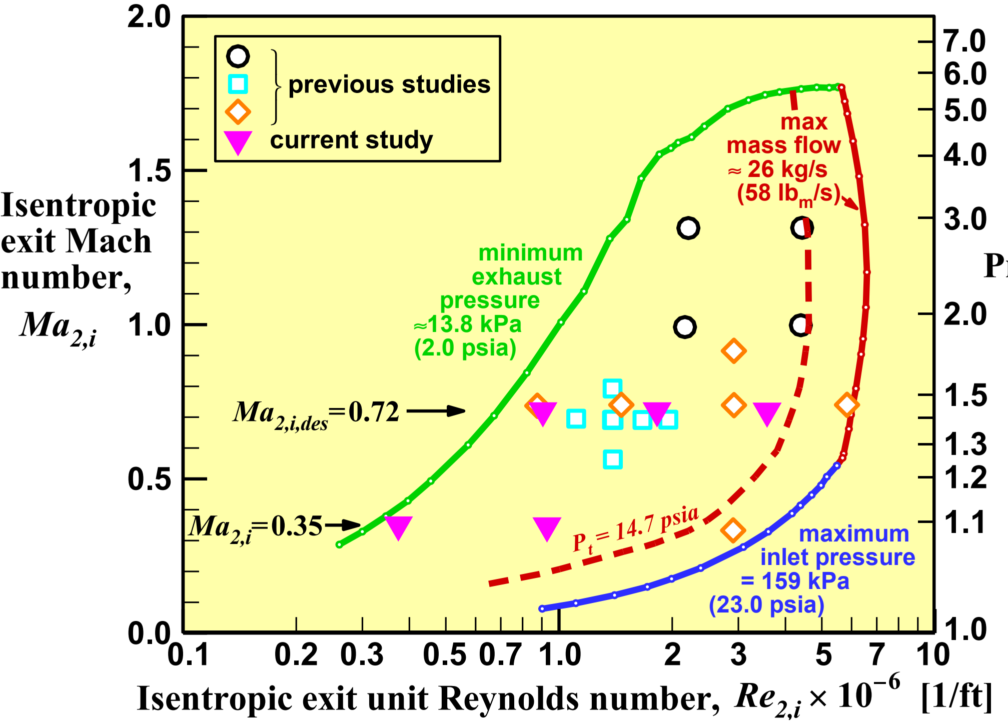

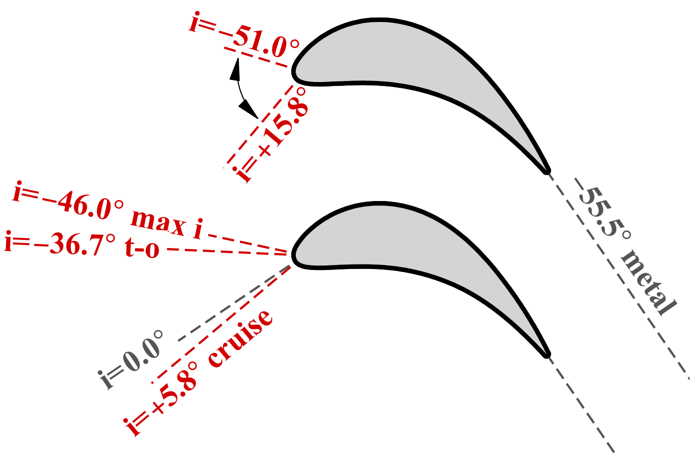

Inlet Angle, β_1	*i*	*Zw*	Facility
50.0°	15.8°	1.22	NASA
45.0°	10.8°	1.13	NASA
40.0° (Cruise)	5.8°	1.06	both
34.2°	0.0°	0.99	both
28.0°	−6.2°	0.92	both
18.1°	−16.1°	0.82	both
8.2°	−26.0°	0.74	both
−2.5° (Takeoff)	−36.7°	0.65	both
−11.8° (max mission *i*)	−46.0°	0.58	both
−16.8°	−51.0°	0.53	both

Experimental Facilities

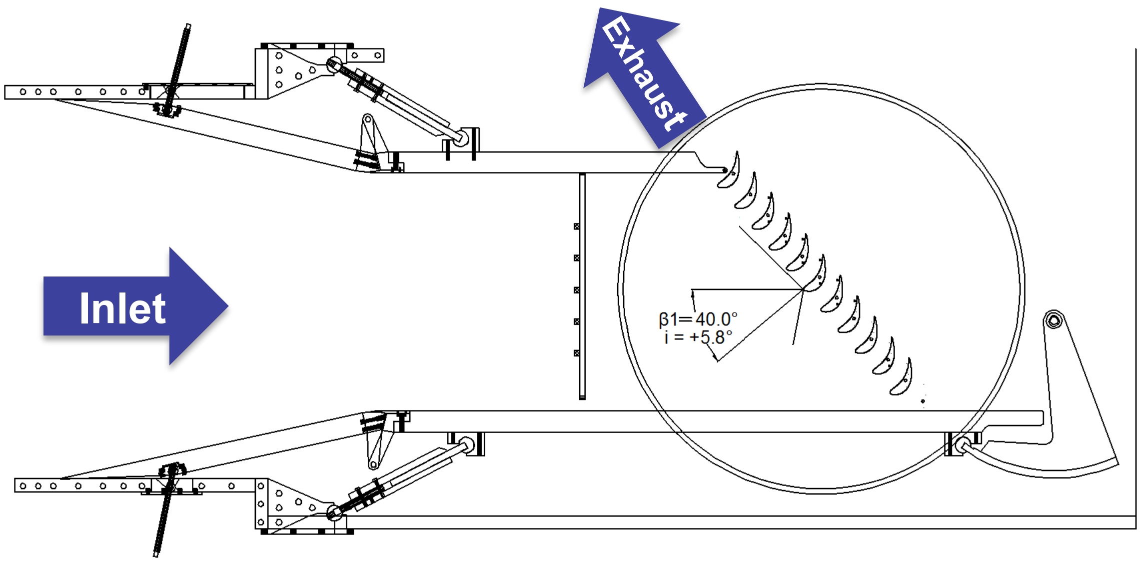

NASA Transonic Turbine Blade Cascade

Flow Parameters	
Exit Re_{Cx}	Exit Ma_{is}
2.12×10^6 ($4.0 \bullet Re_b$)	0.72
1.06×10^6 ($2.0 \bullet Re_b$)	0.72
5.30×10^5 ($1.0 \bullet Re_b$)	0.72
5.30×10^5 ($1.0 \bullet Re_b$)	0.35
2.12×10^5 ($0.4 \bullet Re_b$)	0.35

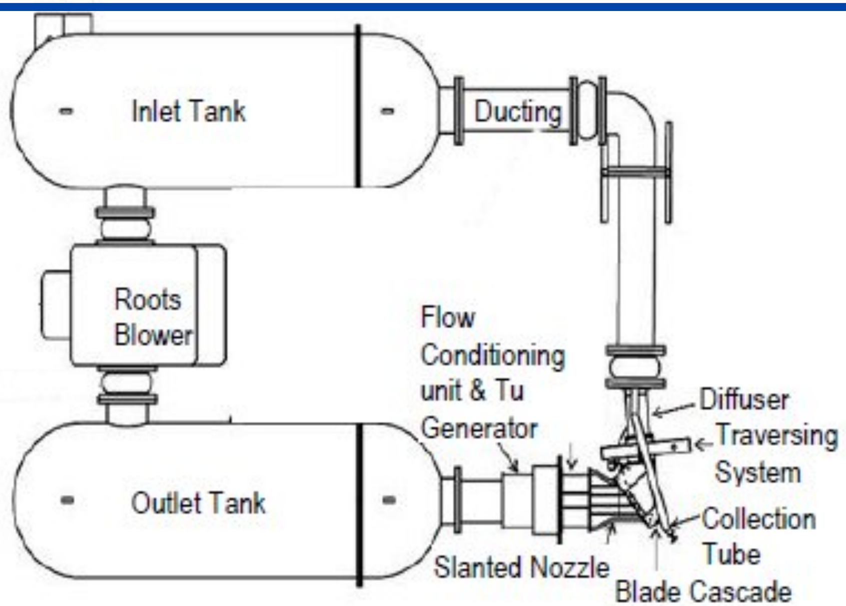

UND Compressible Flow Facility

Flow Parameters	
Exit Re_{Cx}	Exit Ma_{is}
5.27×10^5 ($1.00 \bullet Re_b$)	0.72
2.12×10^5 ($0.40 \bullet Re_b$)	0.72
6.12×10^4 ($0.12 \bullet Re_b$)	0.72
4.64×10^4 ($0.09 \bullet Re_b$)	0.72
5.27×10^5 ($1.00 \bullet Re_b$)	0.35
2.12×10^5 ($0.40 \bullet Re_b$)	0.35

Test Configurations

NASA

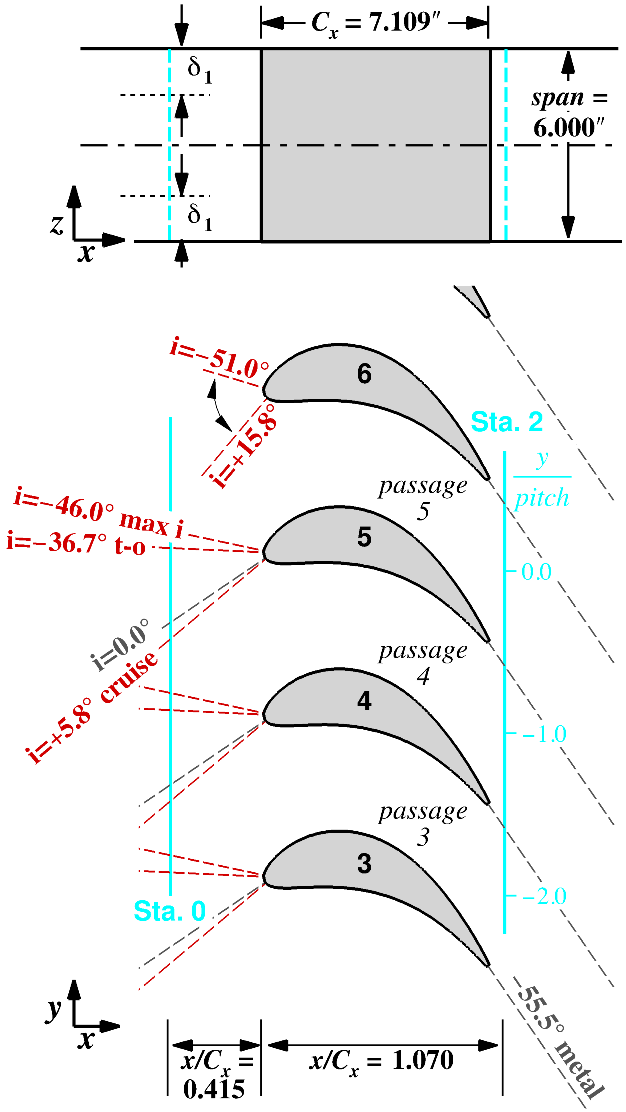

UND

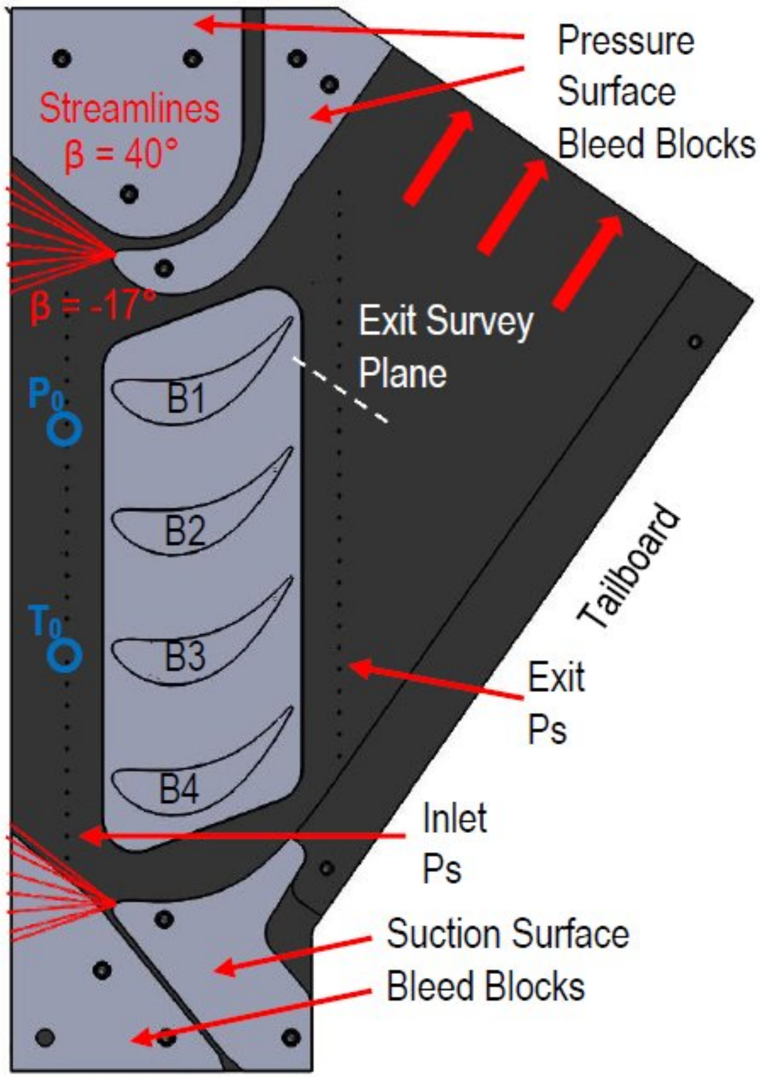

Blade and Inlet Parameters

Blade Parameters		
Parameter	NASA Value	UND Value
Axial Chord, C_x [inch]	7.109	2.673
True Chord [inch]	7.655	2.878
Pitch, S [inch]	5.119	1.925
Span, H [inch]	6.000	2.000
Solidity, C_x/S	1.389	1.388
Aspect Ratio, H/C_x	0.844	0.748
Throat Dimension [inch]	2.868	1.062
Stagger Angle [deg.]	20.35°	20.35°
Inlet Metal Angle [deg.]	34.2°	34.2°
Uncovered Turning deg.]	19.47°	19.47°
Exit Metal Angle [deg.]	−55.54°	−55.54°

Inlet Flow Parameters

NASA	Inlet Tu	$\frac{\delta}{(span/2)}$
low Tu	0.24% - 0.40%	39% - 56%
high Tu	8% - 15%	19% - 29%

UND	Inlet Tu	$\frac{\delta}{(span/2)}$
low Tu	0.32% - 0.42%	3% - 10%
high Tu	3.4% - 4.5%	7% - 11%

Notes: NASA inlet boundary thickness estimated from inlet Reynolds number scaling.
UND inlet boundary layer thickness estimated from power-law assumption from θ measurements.

BLADE LOADING MEASUREMENTS

Blade Loading – Design Incidence

$$Cp_s = \frac{P - \overline{P_2}}{\overline{P_{t,1}} - \overline{P_2}}$$

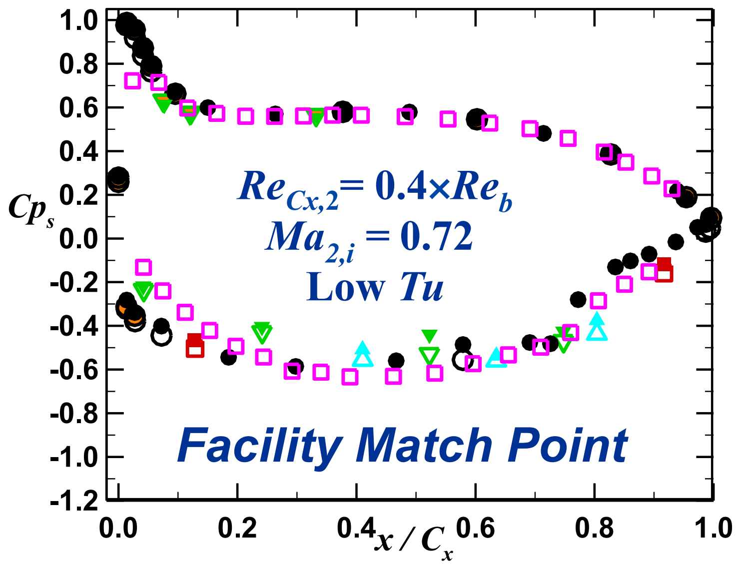

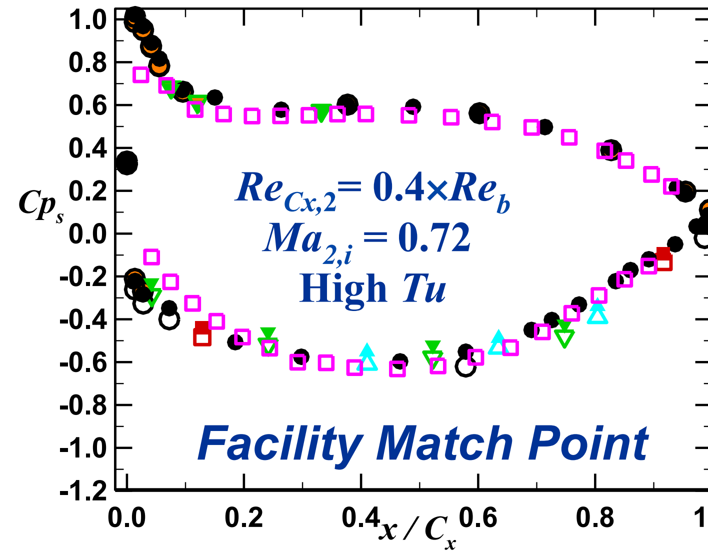

blade	%span
6	50%
6	10%
4	50%
4	30%
4	15%
4	10%
5	50%
5	30%
5	15%
5	10%
UND	50%

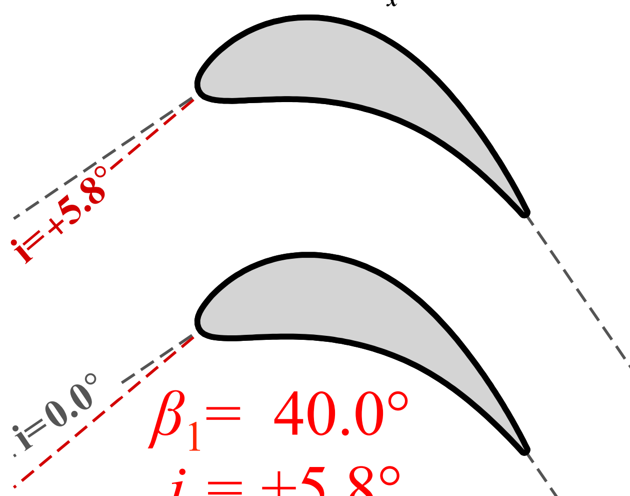

$\beta_1 = 40.0°$
$i = +5.8°$
(Cruise)

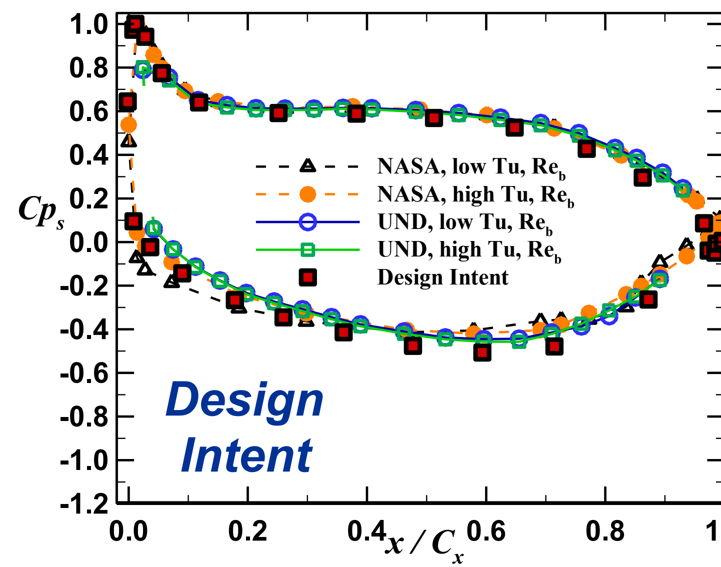

Blade Loading – Highest Negative Incidence

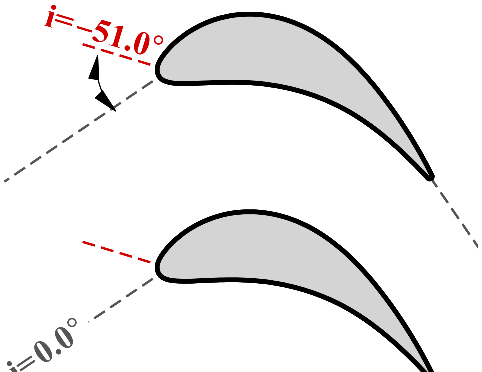

$$\beta_1 = -16.8^\circ$$
$$i = -51.0^\circ$$

$$Cp_s = \frac{P - \overline{P_2}}{P_{t,1} - \overline{P_2}}$$

$Re_{Cx,2}$	$Ma_{2,i}$
$4.0\times Re_b$	0.72
$2.0\times Re_b$	0.72
$1.0\times Re_b$	0.72
$1.0\times Re_b$	0.35
$0.4\times Re_b$	0.35

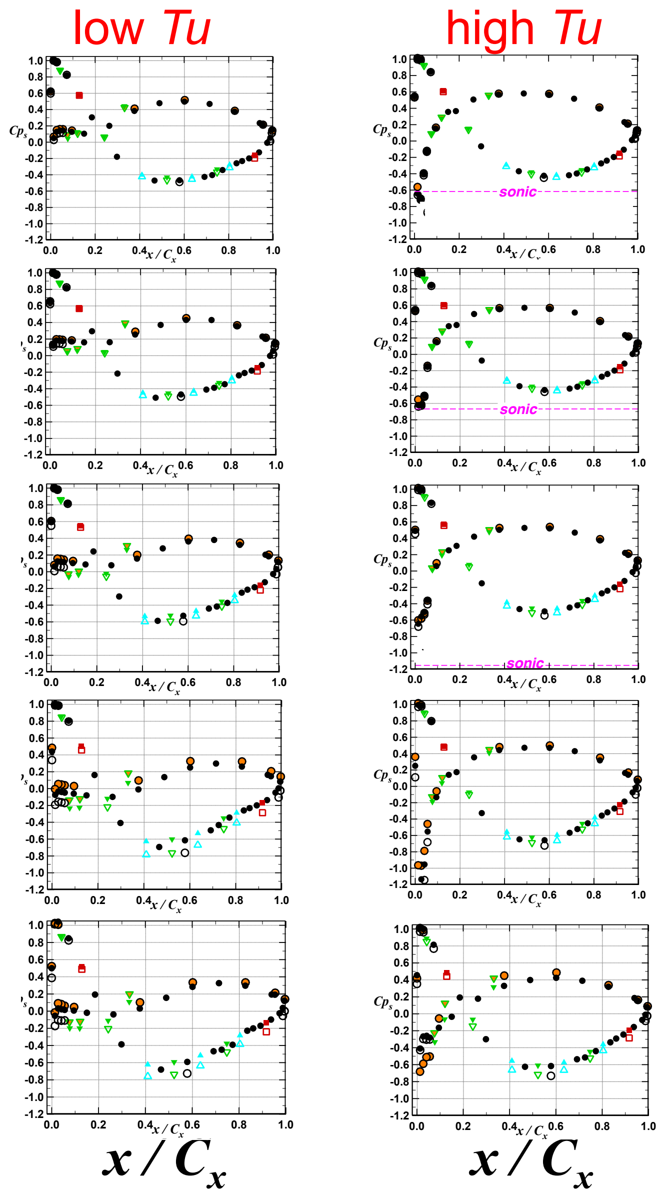

Blade Loading – Effects of Negative Incidence

$$Cp_s = \frac{P - \overline{P_2}}{P_{t,1} - \overline{P_2}}$$

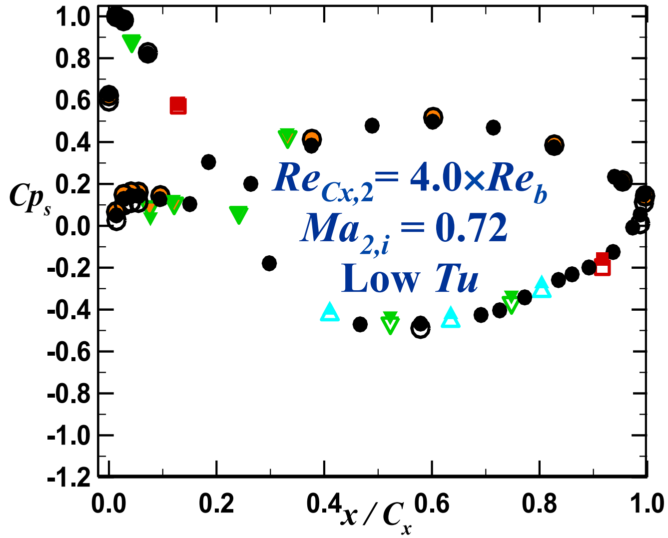

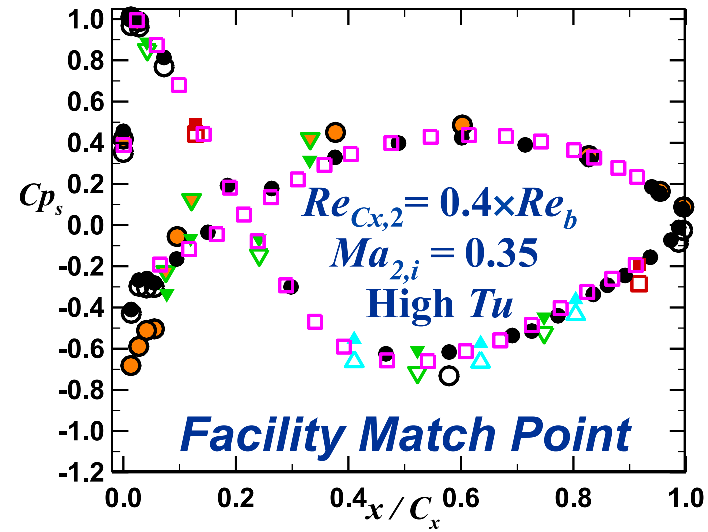

	blade	%span
	6	50%
	6	10%
	4	50%
	4	30%
	4	15%
	4	10%
	5	50%
	5	30%
	5	15%
	5	10%
	UND	50%

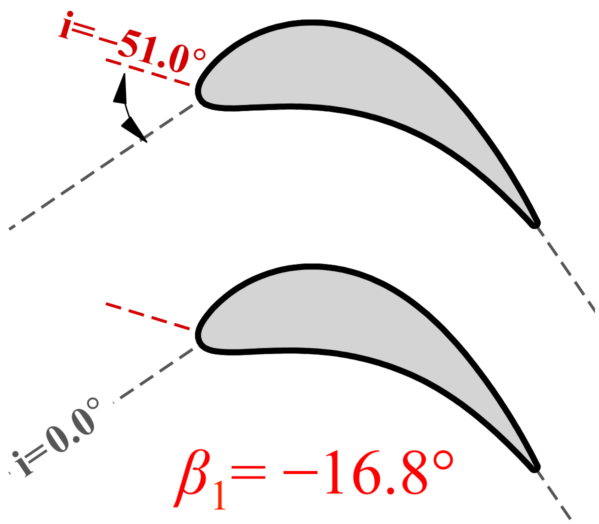

$\beta_1 = -16.8°$
$i = -51.0°$

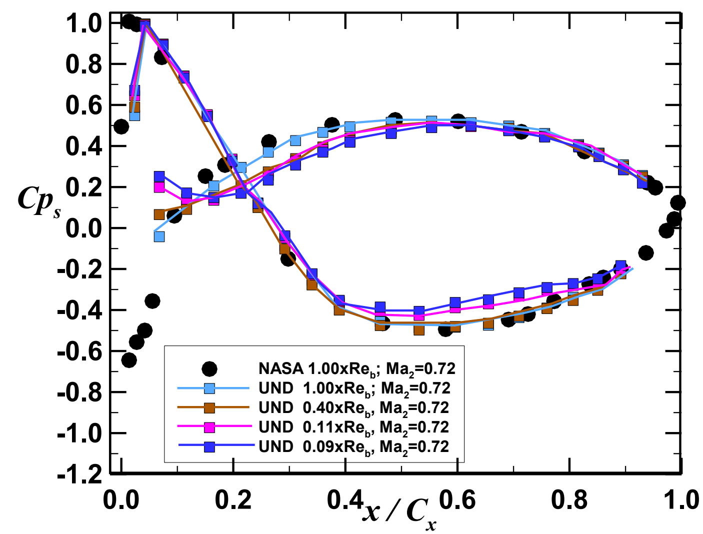

Determination of PS cove separation

HALF-SPAN FLOWFIELD RESULTS

Total Pressure Coefficient Contours and Secondary Flow Vectors

NASA

Re_b; $M_{2,i} = 0.72$; low Tu

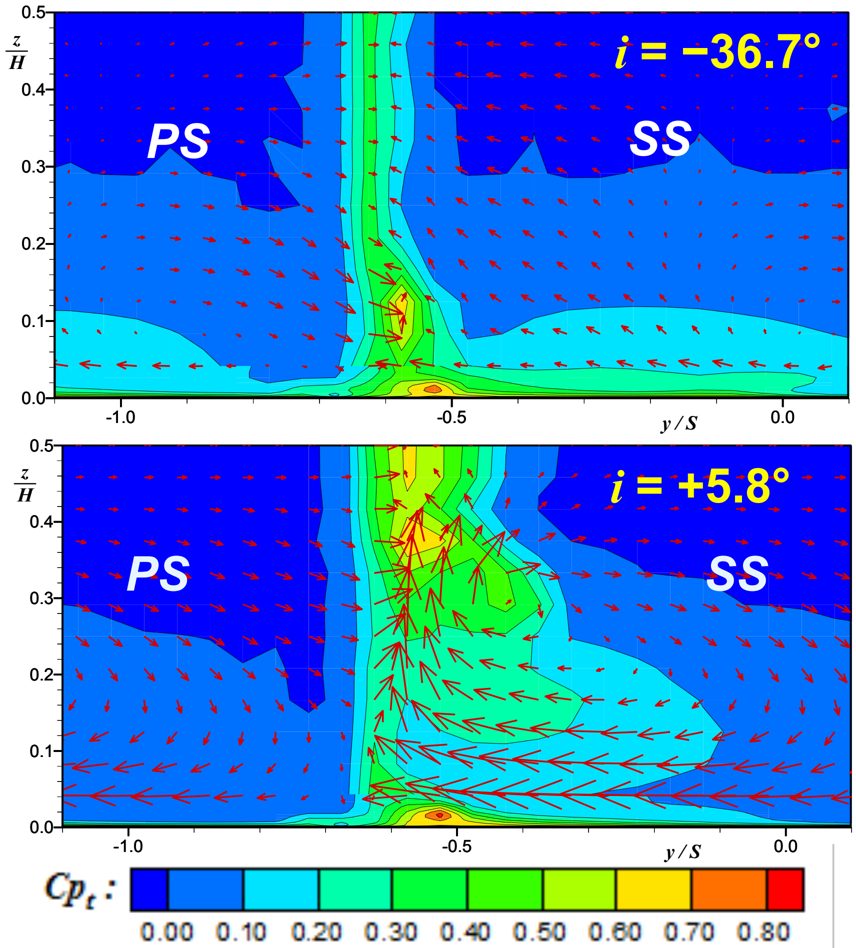

UND

$Re_{Cx,s} = 0.09 \cdot Re_b$; $M_{2,i} = 0.72$; high Tu

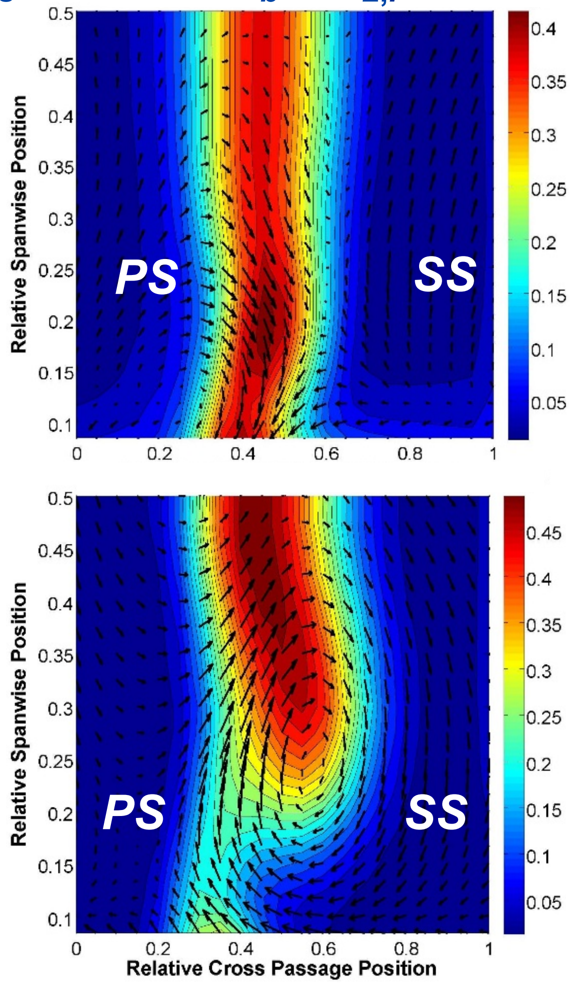

$i = -36.7°$ **(Takeoff)**

$i = +5.8°$ **(Cruise)**

$$Cp_t\,,\ \Omega = \frac{P_{t,1} - P_t}{P_{t,1} - \overline{P_2}}$$

Pitchwise Integrated Data, i = +5.8° (Cruise)

NASA

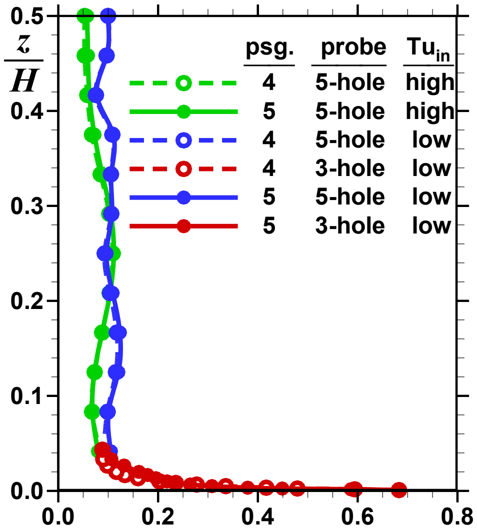

(a) Cp_t (Area Averaged)

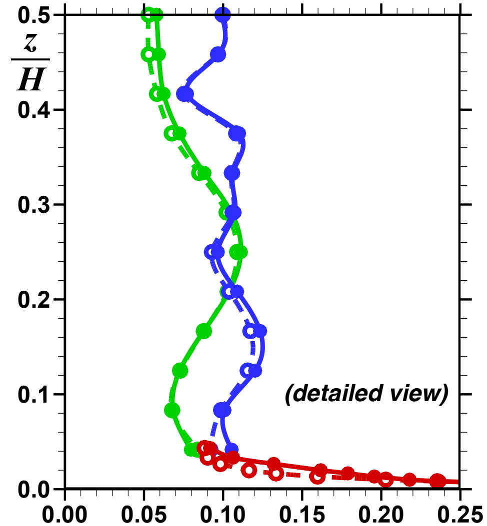

(b) Cp_t (Area Averaged)

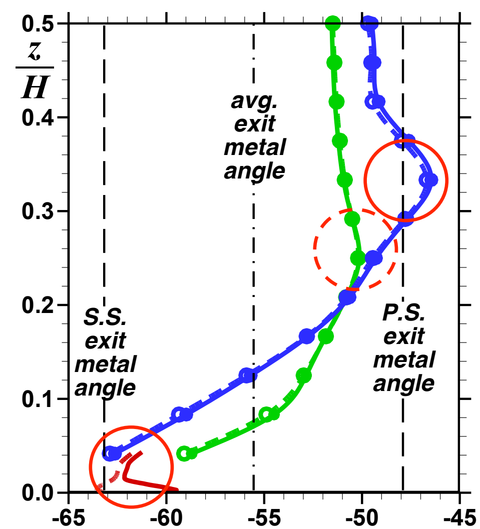

(c) β [deg] (Mass Averaged)

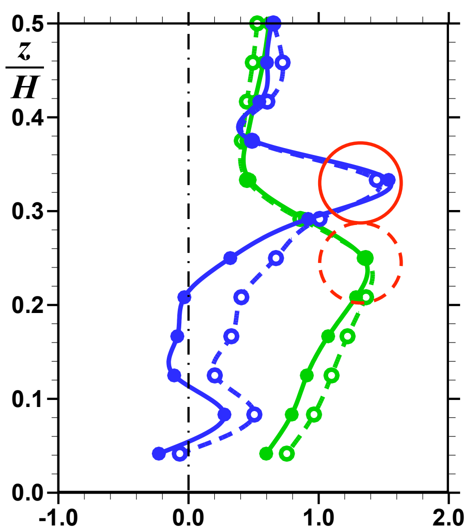

(d) γ [deg] (Mass Averaged)

UND

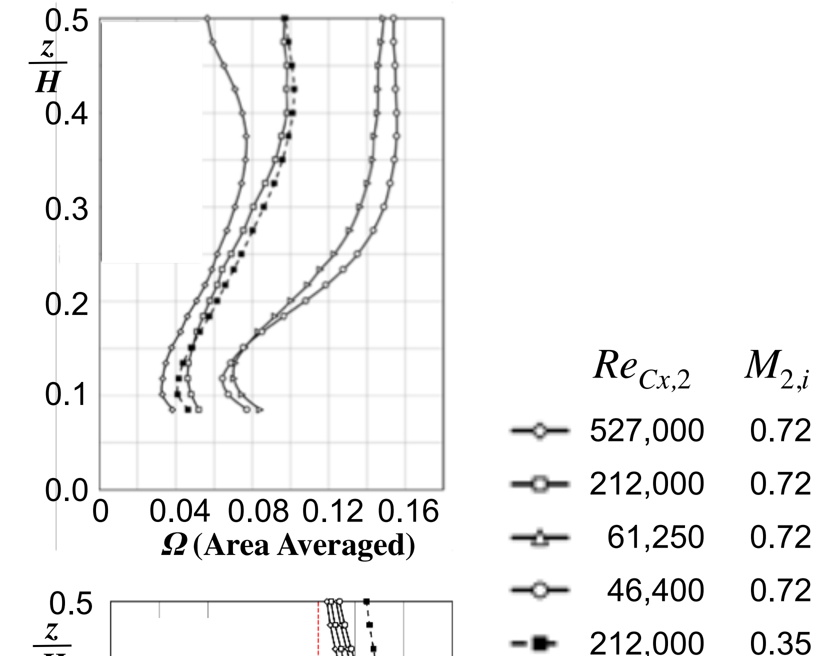

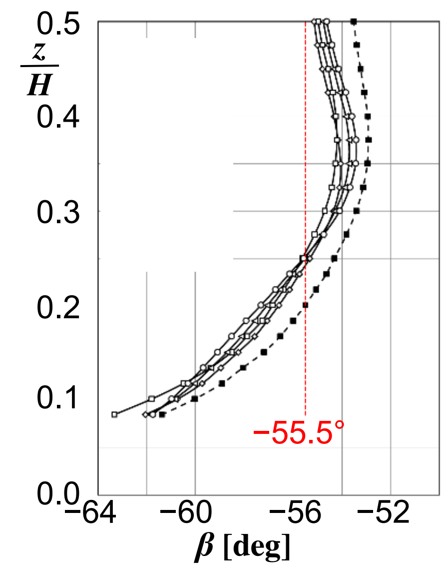

MIDSPAN HEAT TRANSFER MEASUREMENTS

Midspan Stanton Number Distributions

influence of Reynolds number at high Tu

i = +5.8° (Cruise)

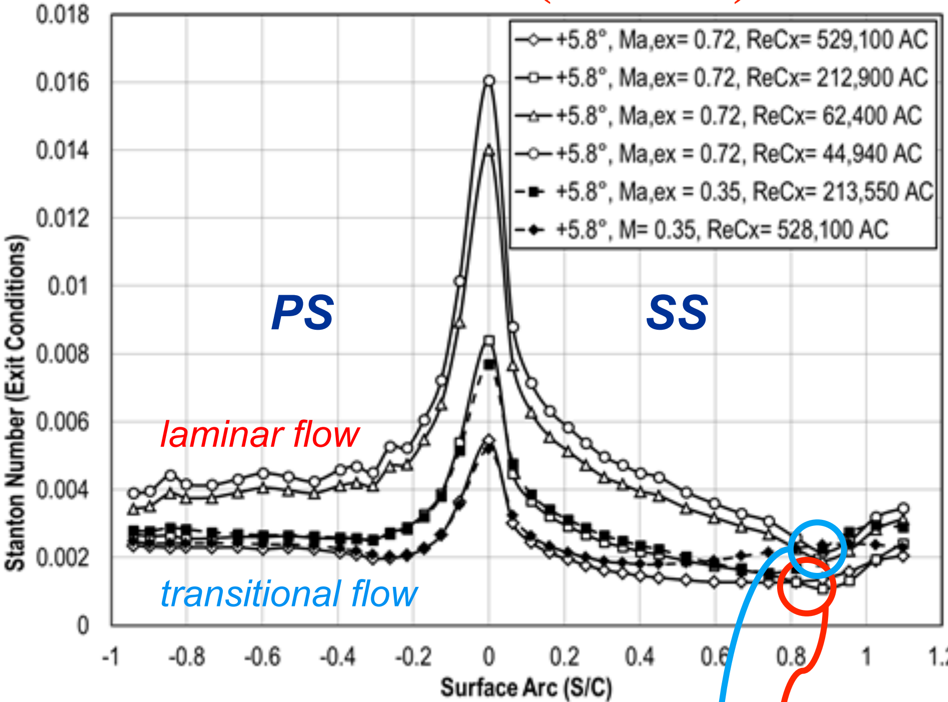

i = −36.8° (Takeoff)

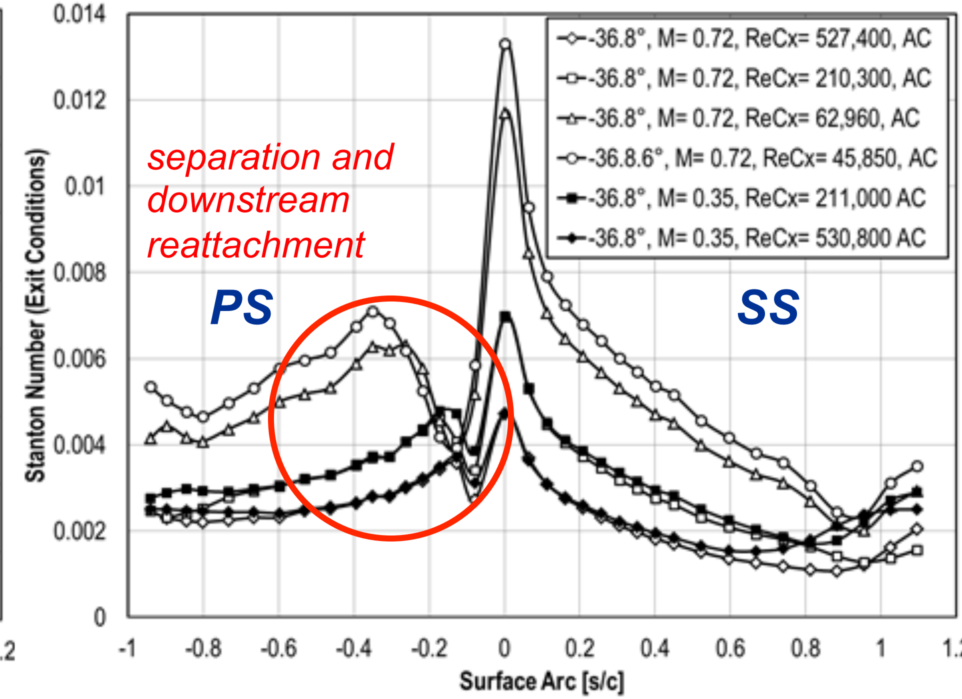

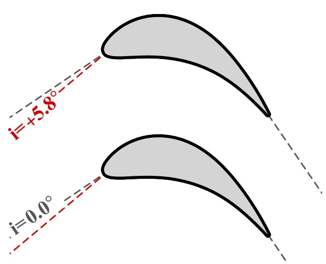

inflection indicates laminar separation.

slope reversal indicates transition start.

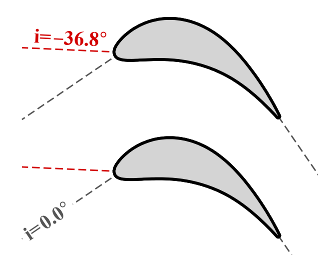

MIDSPAN EXIT SURVEYS

Effects of Reynolds Number and Mach Number at *i* = +5.8°

UND

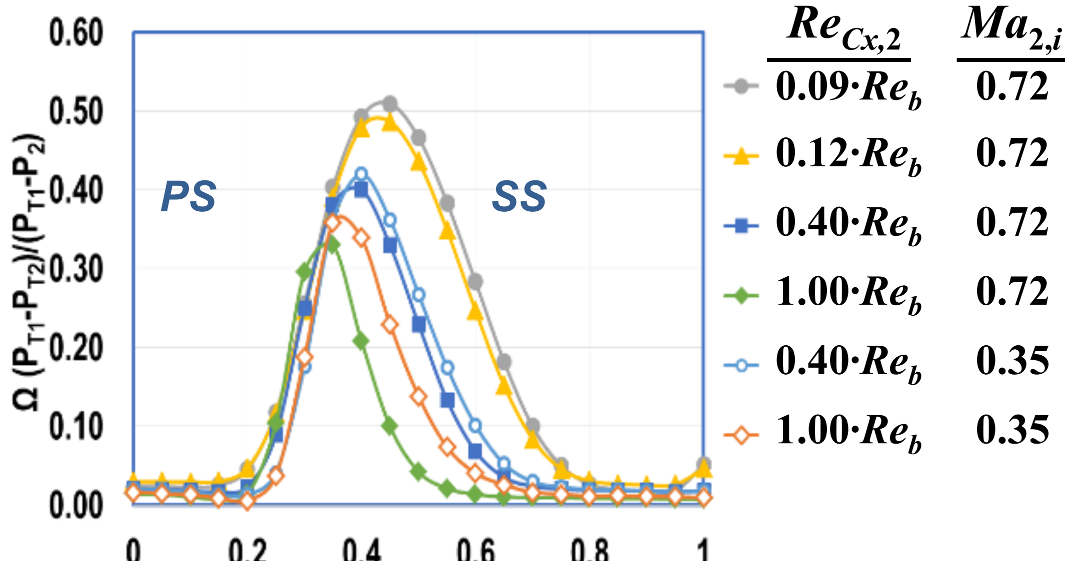

Low *Tu*

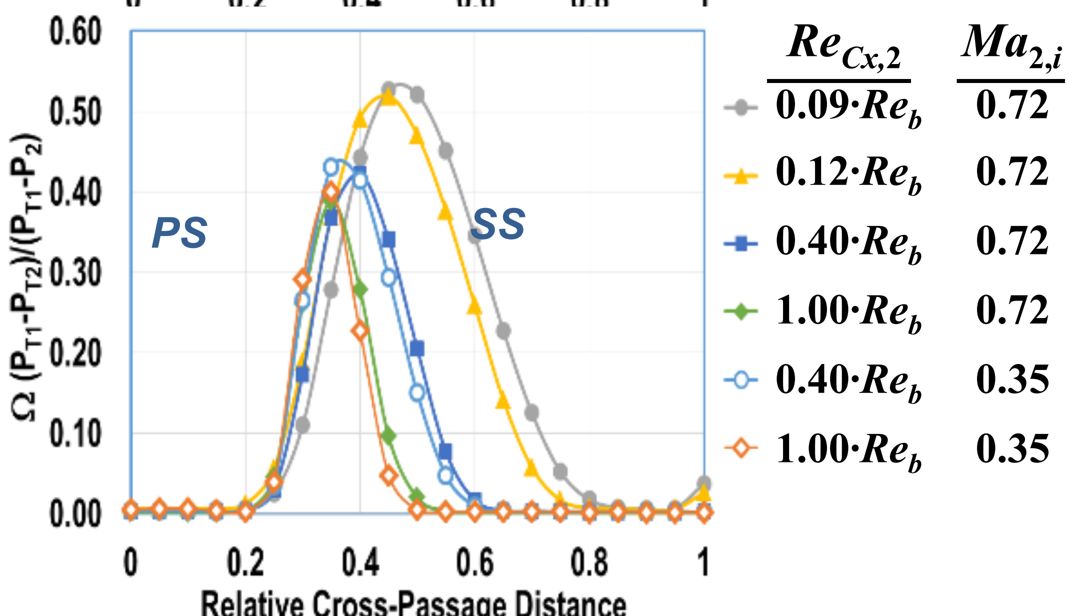

High *Tu*

Effects of Reynolds Number and Mach Number at $i = -51.0°$

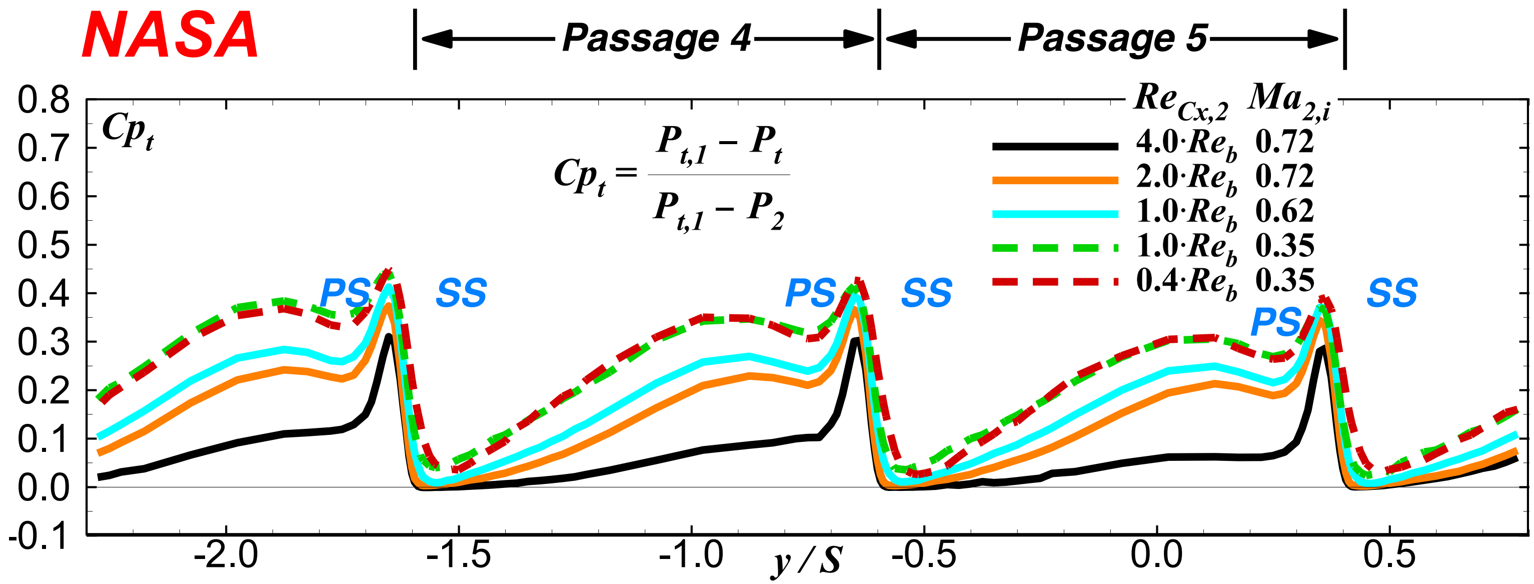

Low *Tu*

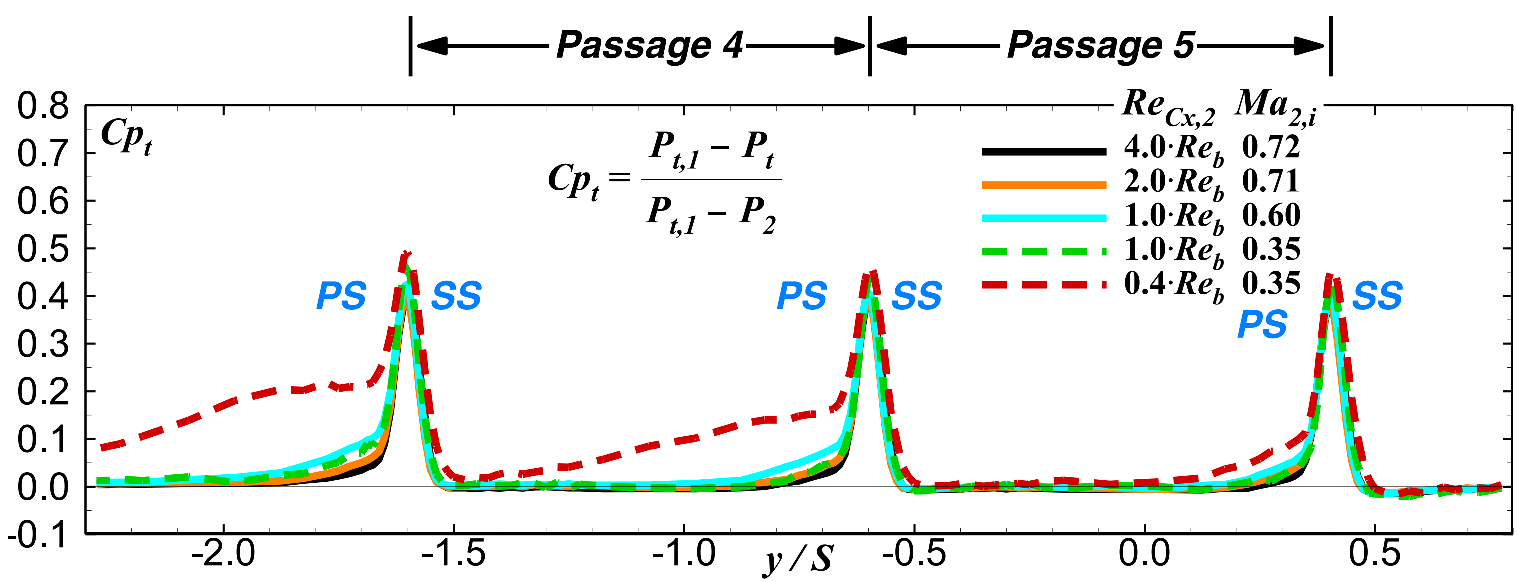

High *Tu*

Effects of Reynolds Number at $Ma_{2,i} = 0.72$, $i = -51.0°$

UND

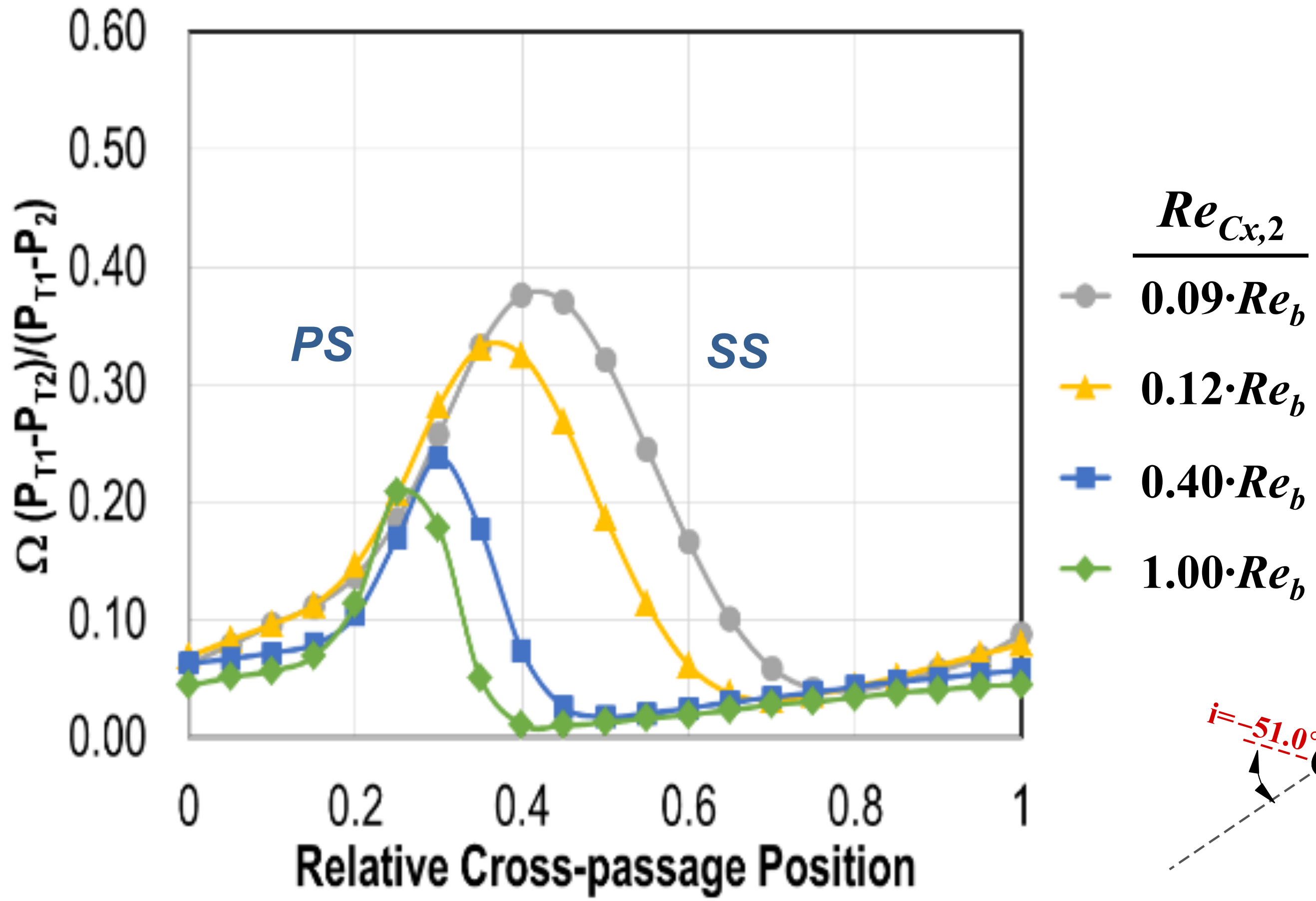

High *Tu*

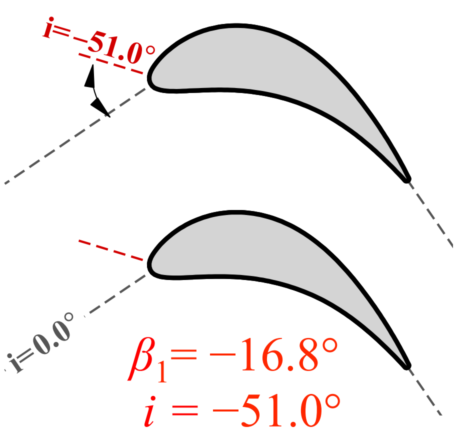

Effects of Inlet Flow Angle

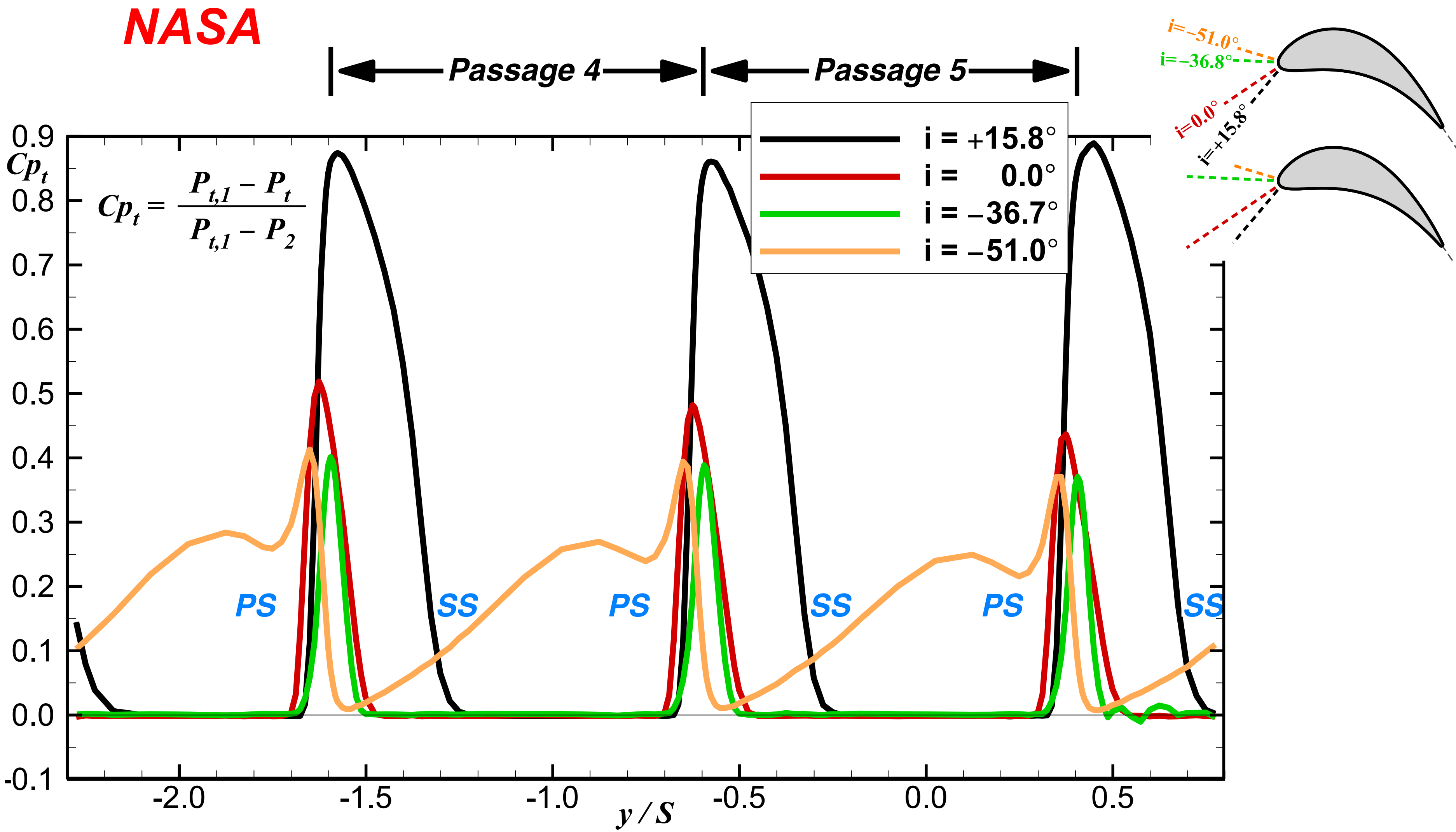

$Re_{Cx,2}$= 5.30 x 10^5 (1.0·Re_b); M_2=0.72; Low *Tu*

Effects of Inlet Flow Angle

UND

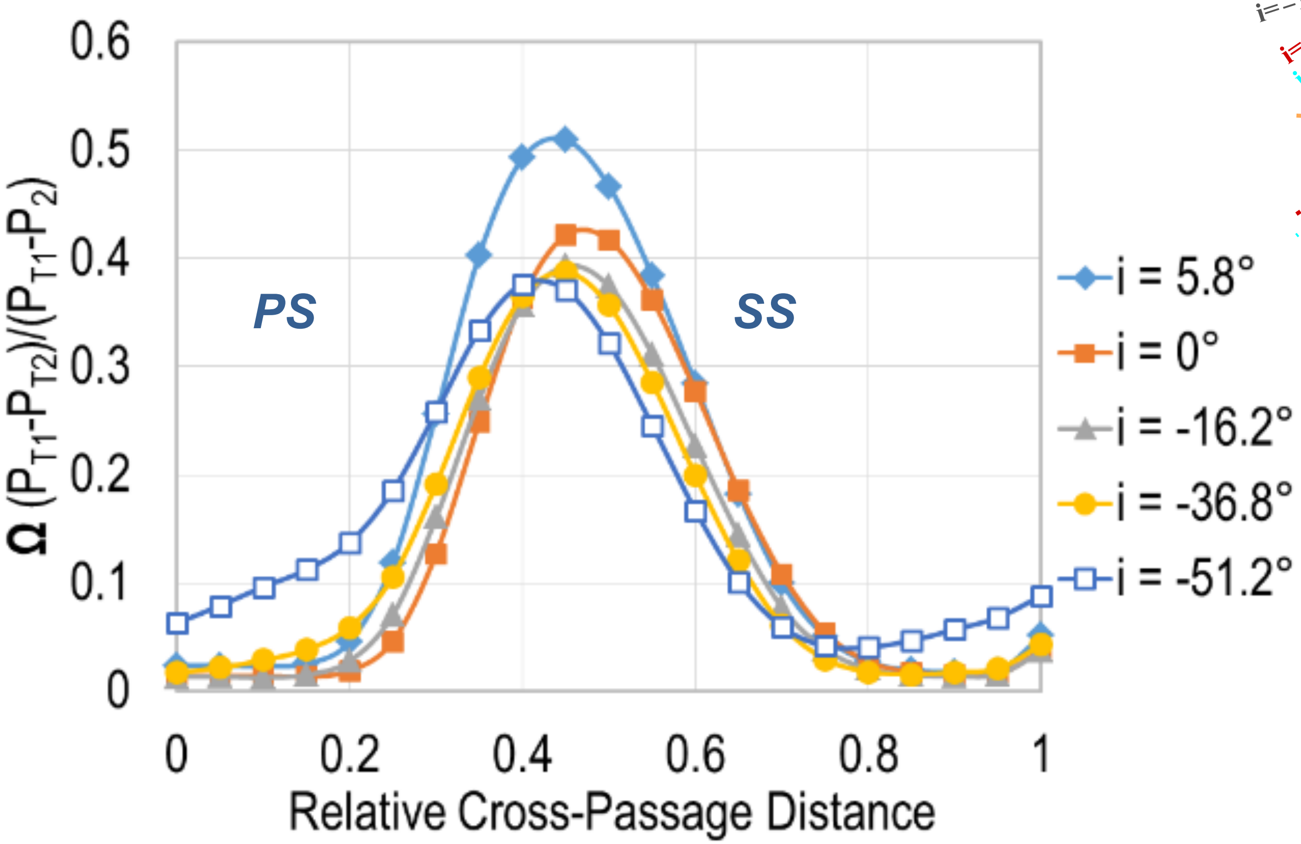

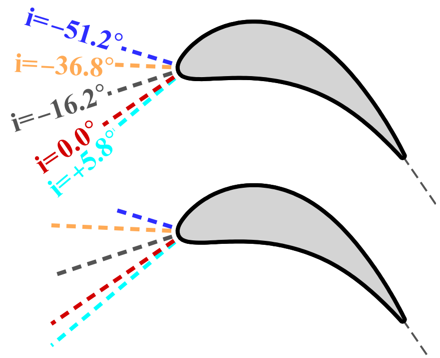

$Re_{Cx,2}$= 4.64 x 10^4 (0.09·Re_b); M_2=0.72; High *Tu*

LOSS BUCKETS

Half-Span Average Loss Buckets

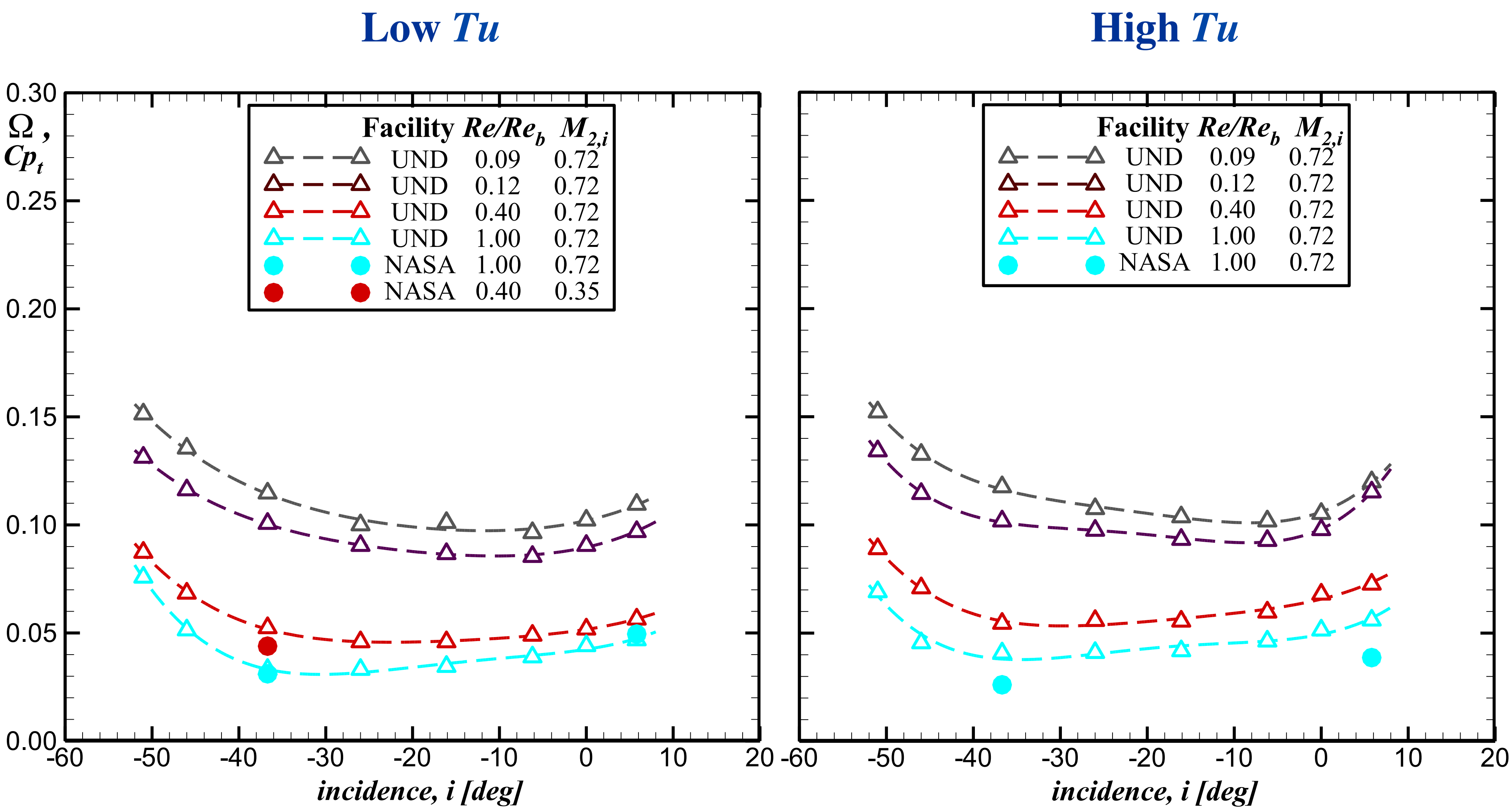

Midspan Loss Buckets

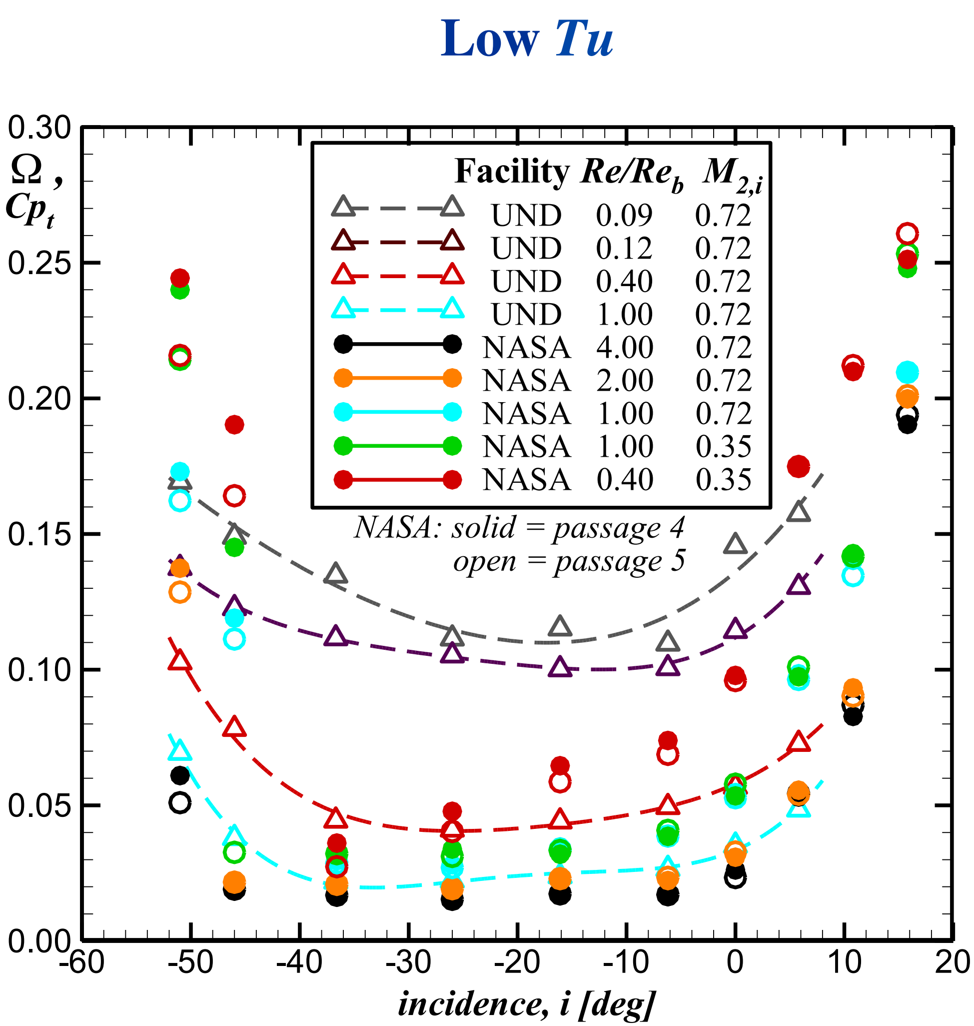

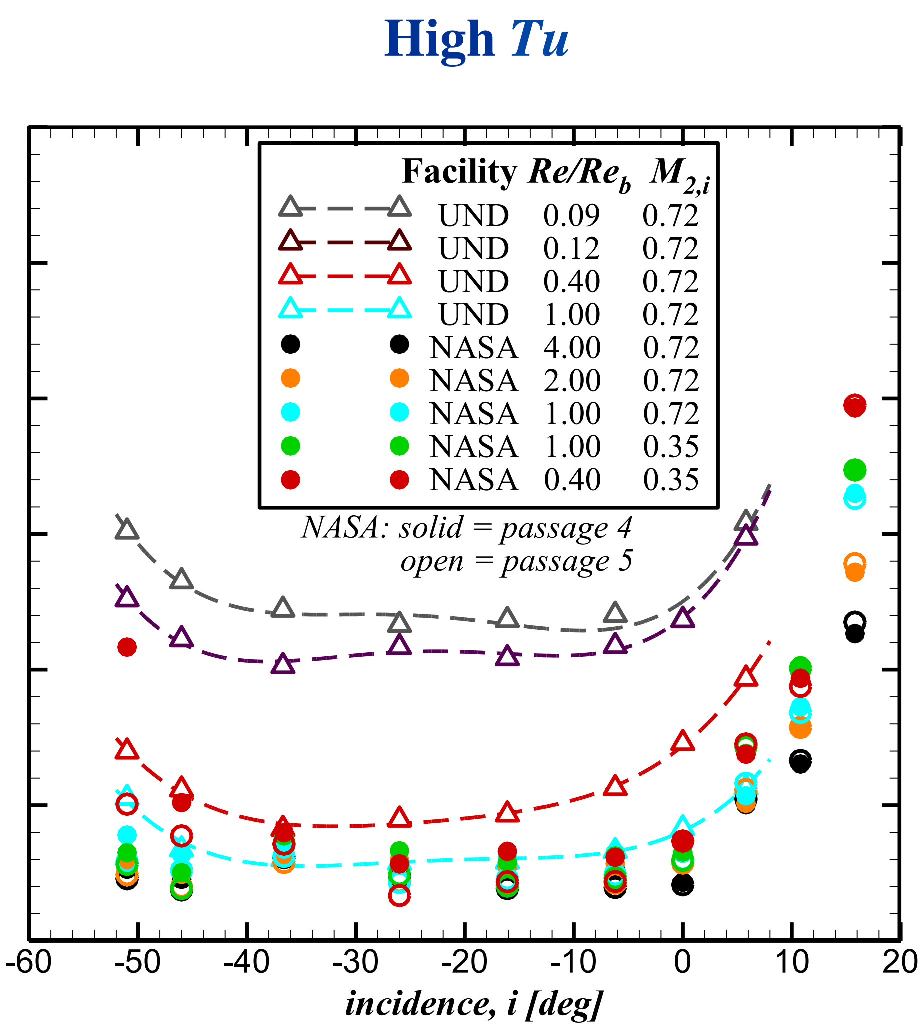

Summary

- Complementary facilities provided data over a wider range of flow conditions:
  - NASA's larger scale provided higher Reynolds number data;
  - UND's smaller scale provided lower Reynolds number data and match points.

- Data highlighted the effects of:
  - Reynolds number;
  - Exit Mach number;
  - Inlet turbulence levels;
  - Wide incidence range;
  - Relative inlet boundary layer thickness;
- On the following:
  - Blade loading;
  - Wake profiles;
  - Blade row loss levels;
  - Blade row turning levels;
  - Blade surface boundary layer state;
  - Exit flow field characteristics.

NASA

Midspan Loss Buckets

Low *Tu*

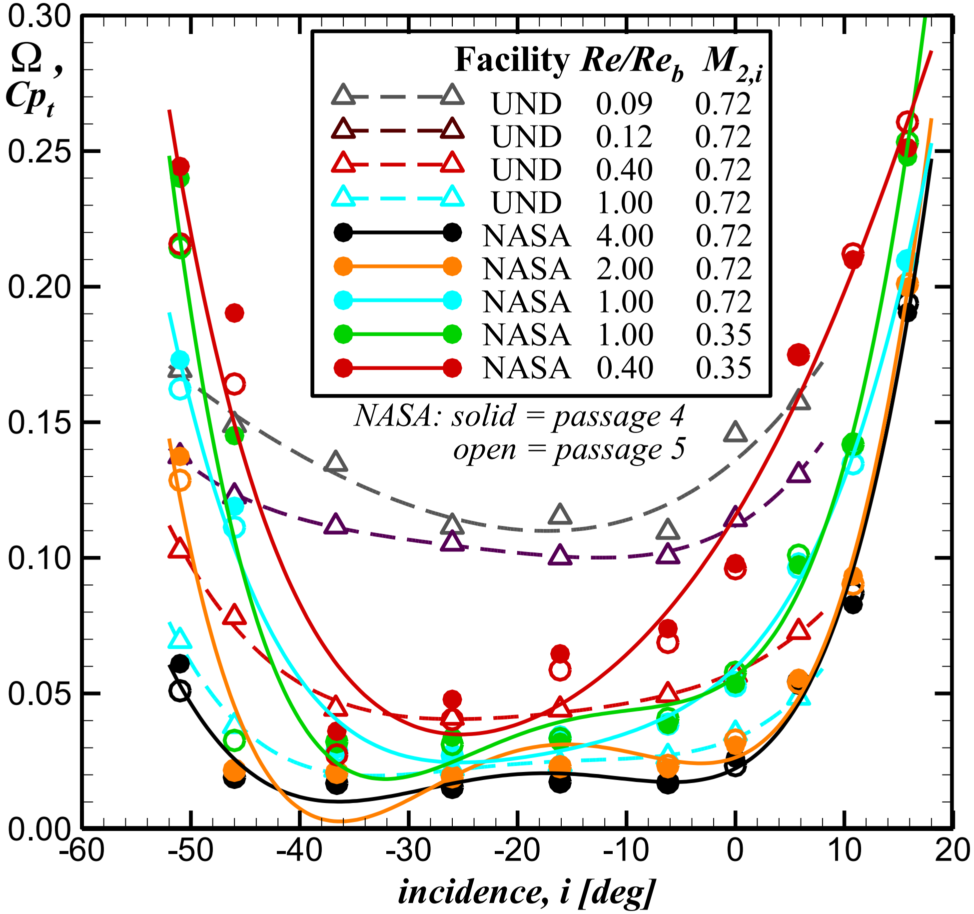

High *Tu*

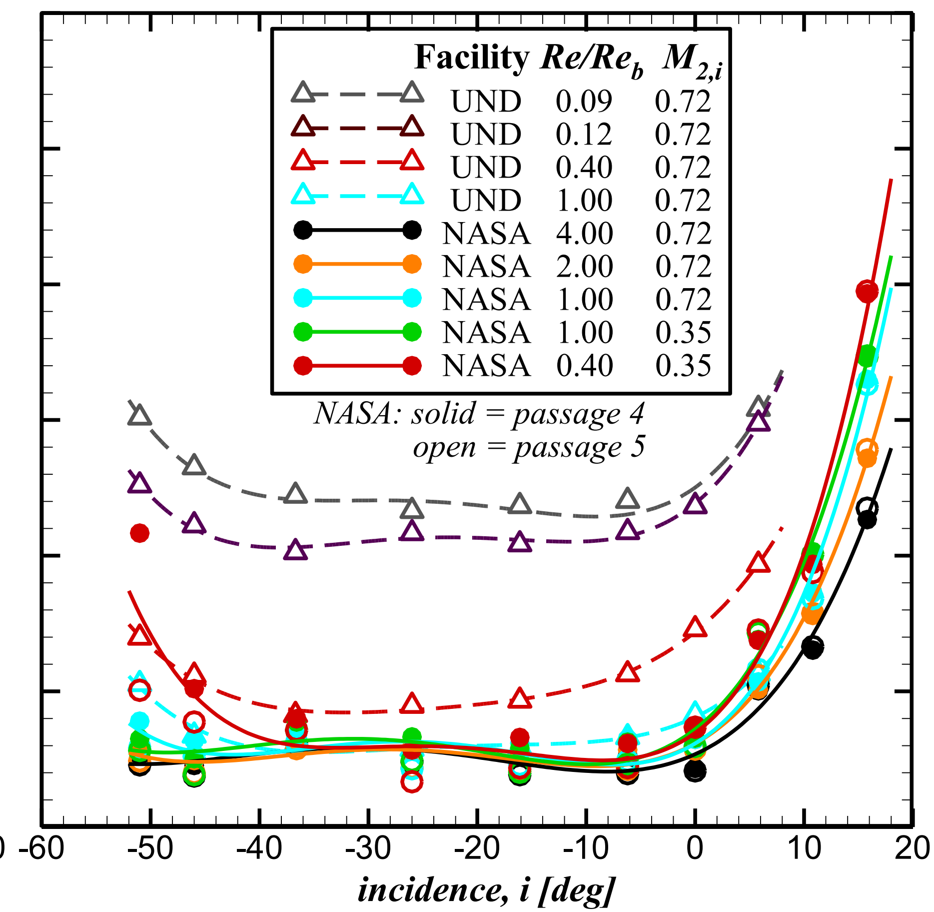

Midspan Loss Scaling

Low *Tu*

$Re^{-0.5}$ Scaled Loss Bucket

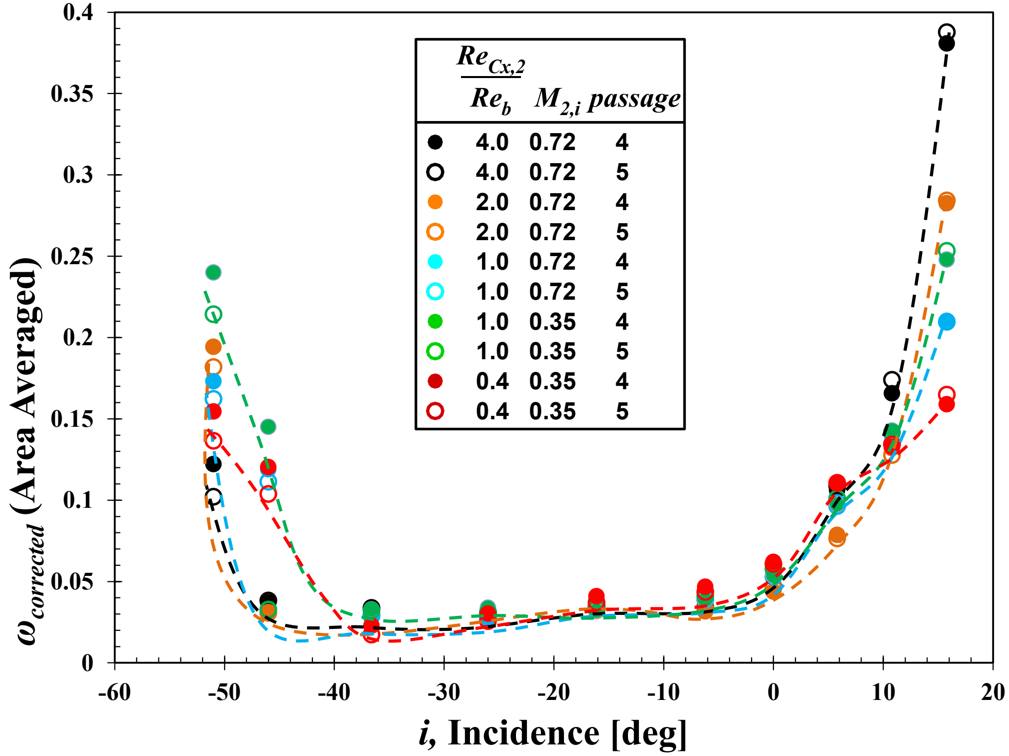

High *Tu*

$Re^{-0.1}$ Scaled Loss Bucket

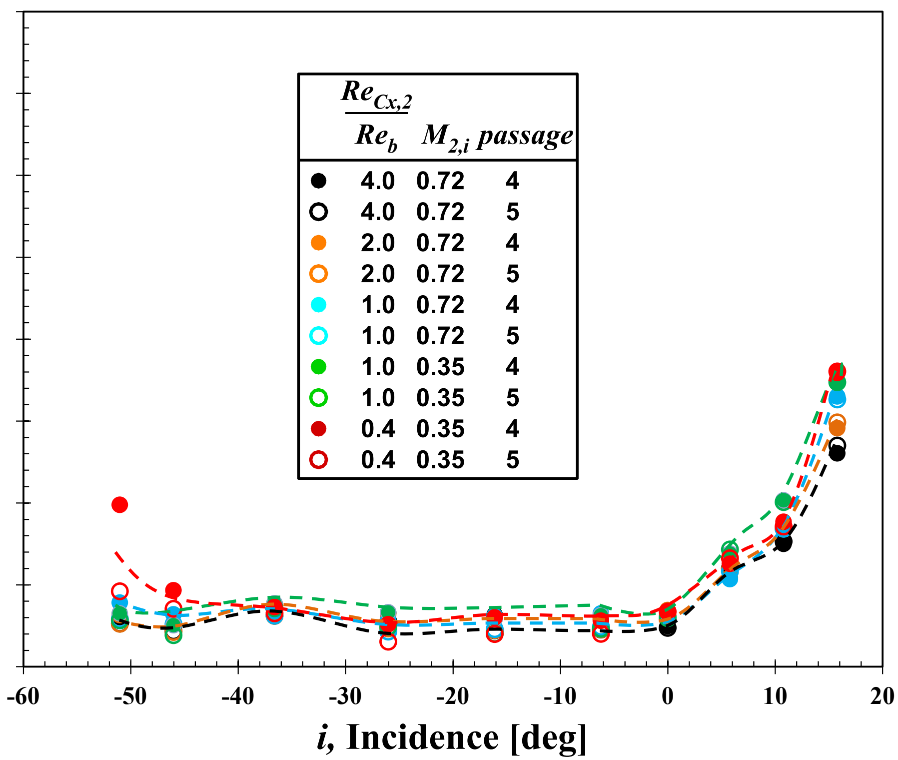

Ainley-Mathieson Midspan Loss Scaling

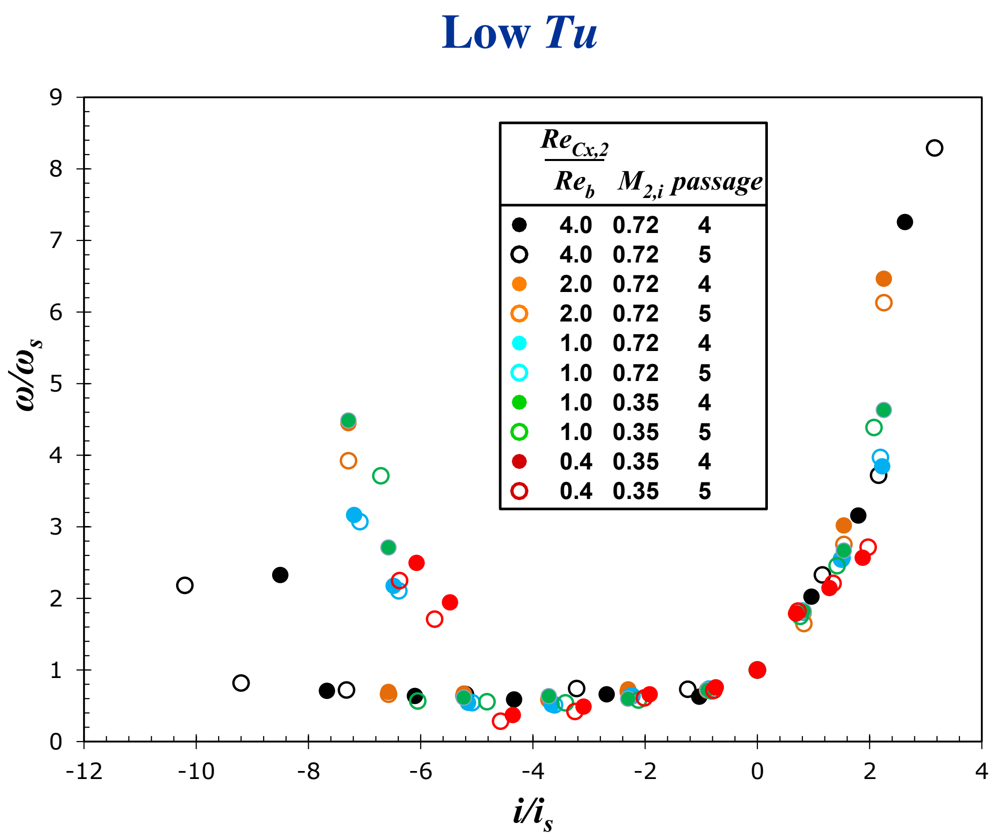

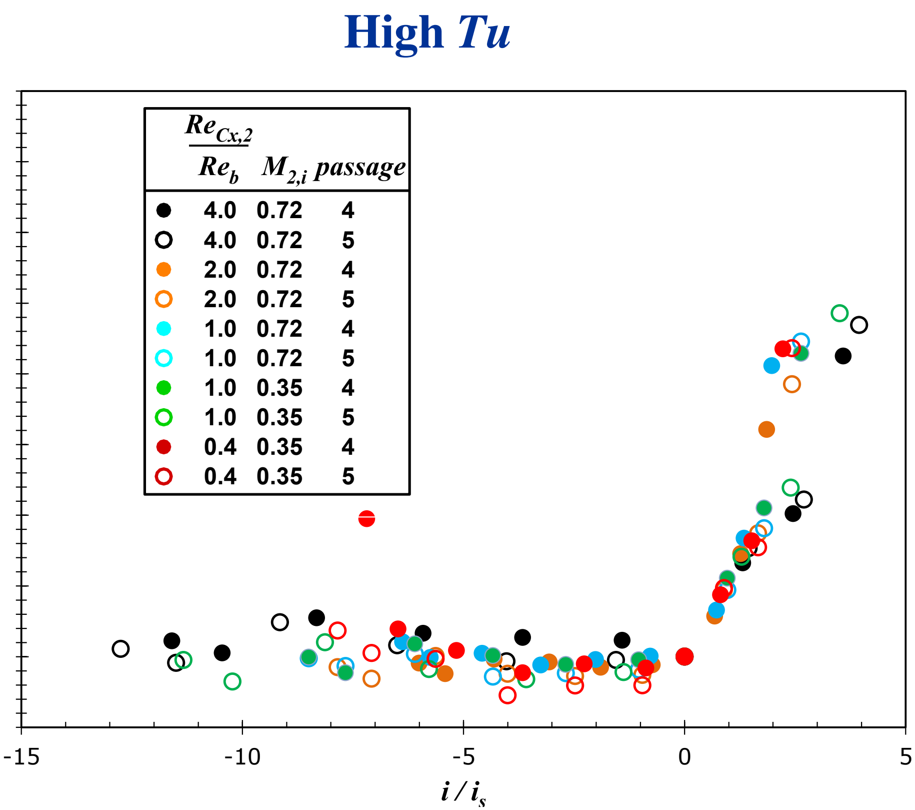

Exit Flow Angles

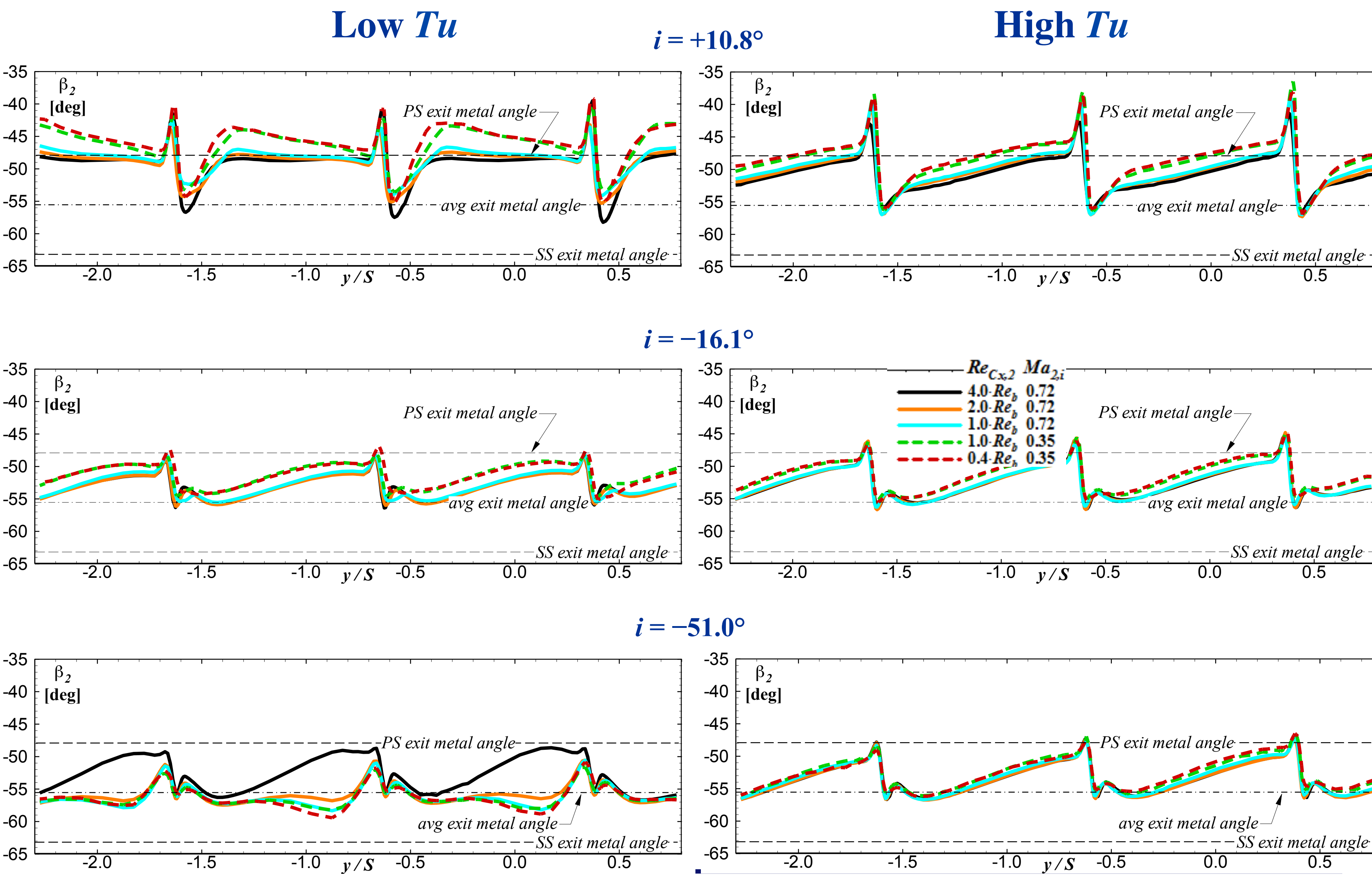

Average Exit Flow Angle

Low *Tu*

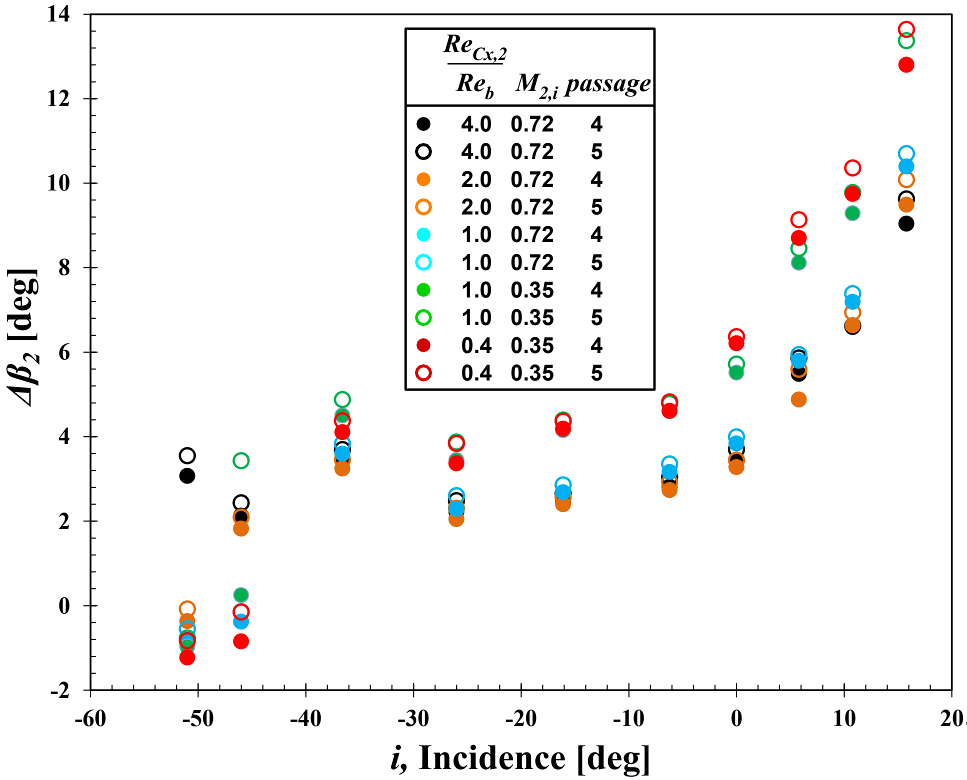

High *Tu*

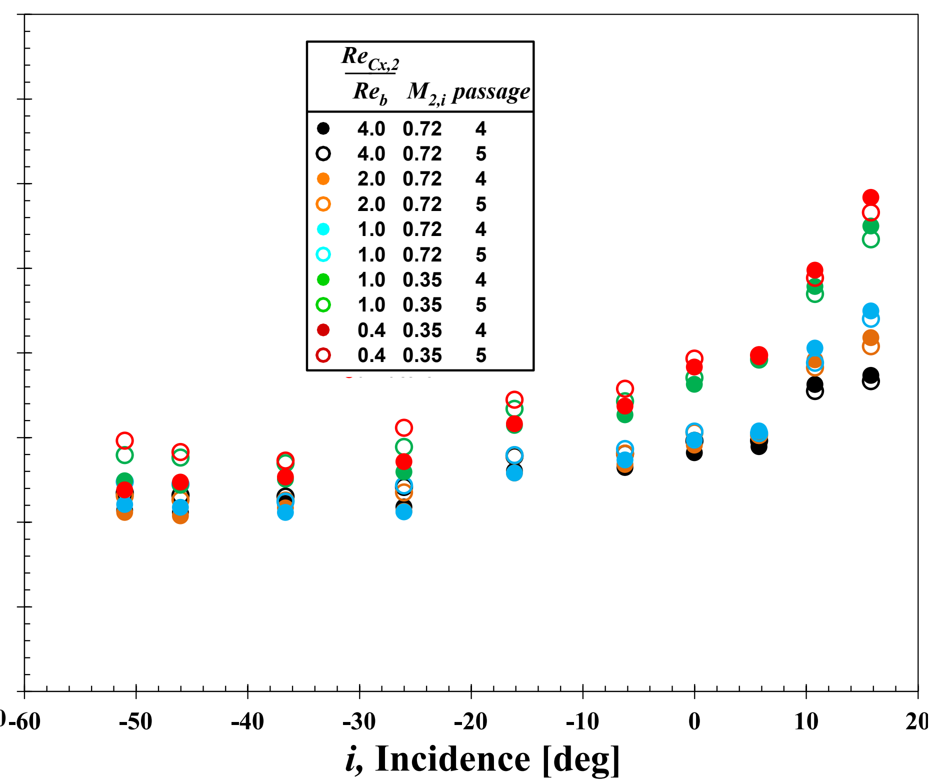

$$\Delta\beta_2 = \beta_2 + 55.54°$$